HHS Public Access

Author manuscript

J Med Genet. Author manuscript; available in PMC 2019 July 01.

Published in final edited form as:

J Med Genet. 2018 July ; 55(7): 479–488. doi:10.1136/jmedgenet-2017-105221.

Inframe deletion of human *ESPN* is associated with deafness, vestibulopathy and vision impairment

Zubair M Ahmed[1], **Thomas J Jaworek**[#1], **Gowri N Sarangdhar**[#2], **Lili Zheng**[3], **Khitab Gul**[2], **Shaheen N Khan**[4], **Thomas B Friedman**[5], **Robert A Sisk**[2,6], **James R Bartles**[3], **Sheikh Riazuddin**[7,8], and **Saima Riazuddin**[1,7]

[1]Department of Otorhinolaryngology Head and Neck Surgery, School of Medicine, University of Maryland, Baltimore, Maryland, USA

[2]Abrahamson Pediatric Eye Institute, Cincinnati Children's Hospital, Cincinnati, Ohio, USA

[3]Department of Cell and Molecular Biology, School of Medicine, Northwestern University Feinberg, Chicago, Illinois, USA

[4]Center for Excellence in Molecular Biology, University of the Punjab, Lahore, Pakistan

[5]Laboratory of Molecular Genetics, National Institute on Deafness and Other Communication Disorder, National Institutes of Health, Bethesda, Maryland, USA

[6]Ophthalmology, Cincinnati Eye Institute, Cincinnati, Ohio, USA

[7]Shaheed Zulfiqar Ali Bhutto Medical University, Islamabad, Pakistan

[8]University of Lahore and Allama Iqbal Medical Research Centre, Jinnah Hospital Complex, Lahore, Pakistan

[#] These authors contributed equally to this work.

Correspondence to Professor Zubair M Ahmed, Department of Otorhinolaryngology Head and Neck Surgery, University of Maryland School of Medicine, Baltimore, MD 21201, USA; zmahmed@som.umaryland.edu.

Contributors ZMA and SaR conceived and designed the study. ZMA, TJJ, GNS, KG, LZ and JRB performed experiments. ZMA, TJJ, LZ, RAS, GNS, KG and JRB analysed data. SNK, ShR and TBF ascertained the family and contributed reagents and materials. ZMA, TJJ, GNS, LZ, JRB and SaR prepared the figures. ZMA and SaR wrote the paper, and all the coauthors edited the manuscript and approved final submission.

Additional material is published online only. To view please visit the journal online .(http://dx.doi.org/10.1136/jmedgenet-2017-105221).

Web resources
1000 Genomes: http://www.1000genomes.org
Exome Variant Server: http://evs.gs.washington.edu/EVS
MutationTaster: http://www.mutationtaster.org
Online Mendelian Inheritance in Man (OMIM): http://www.omim.org
UCSC Genome Bioinformatics: http://genome.ucsc.edu
Marshfield genetic map: http://research.marshfieldclinic.org.

Competing interests None declared.

Patient consent Obtained.

Ethics approval Approval for this study was obtained from the following institutional review boards (IRBS): the National Centre of Excellence in Molecular Biology, University of the Punjab, Lahore, Pakistan, the Combined Neuroscience Institutional Review Board (OH-93-N-016) and the University of Maryland School of Medicine, USA (HP-00061036).

Provenance and peer review Not commissioned; externally peer reviewed.

Data sharing statement Variant found in PKDF1051 has been deposited in ClinVar database.

Abstract

Background—Usher syndrome (USH) is a neurosensory disorder characterised by deafness, variable vestibular areflexia and vision loss. The aim of the study was to identify the genetic defect in a Pakistani family (PKDF1051) segregating USH.

Methods—Genome-wide linkage analysis was performed by using an Illumina linkage array followed by Sanger and exome seguencing. Heterologous cells and mouse organ of Corti explant-based transfection assays were used for functional evaluations. Detailed clinical evaluations were performed to characterise the USH phenotype.

Results—Through homozygosity mapping, we genetically linked the USH phenotype segregating in family PKDF1051 to markers on chromosome 1 p36.32-p36.22. The locus was designated *USH1M*. Using a combination of Sanger seguencing and exome seguencing, we identified a novel homozygous 18 base pair inframe deletion in *ESPN*. Variants of *ESPN*, encoding the actin-bundling protein espin, have been previously associated with deafness and vestibular areflexia in humans with no apparent visual deficits. Our functional studies in heterologous cells and in mouse organ of Corti explant cultures revealed that the six deleted residues in affected individuals of family PKDF1051 are essential for the actin bundling function of espin demonstrated by ultracentrifugation actin binding and bundling assays. Funduscopic examination of the affected individuals of family PKDF1051 revealed irregular retinal contour, temporal flecks and disc pallor in both eyes. ERG revealed diminished rod photoreceptor function among affected individuals.

Conclusion—Our study uncovers an additional USH gene, assigns the USH1 phenotype to a variant of *ESPN* and provides a 12th molecular component to the USH proteome.

INTRODUCTION

Mammalian vision and hearing necessitate accurate functions of sensory and non-sensory cells. In the inner ear, transcriptome studies of the organ of Corti (OC) revealed the expression of at least 18 133 genes in hair and supporting cells,[1] underscoring the complexity of inner ear development and function. Deficits in the development, patterning or maintenance of inner ear sensory epithelia, especially in neurosensory hair cells, result in hearing loss (HL), a highly variable phenotype that affects over 70 million children worldwide. HL is either the only consistent phenotype (non-syndromic HL) or occurs as one phenotypic feature of a more complex clinical syndrome. There are over 40 syndromes listed in the OMIM database that affect both the auditory and visual systems. Among them, Usher syndrome (USH) is the most common cause of deaf-blindness in school-age children.[2–4]

USH is a neurosensory disorder characterised by partial to total HL, variable vestibular areflexia and vision loss that worsens over time. A molecular diagnosis study suggested a frequency of 1/6000 individuals with USH in the USA.[5] Individuals with USH are often classified as having one of three clinical subtypes. Patients with USH type I (USH1) have profound HL and vestibular dysfunction from birth. In addition, night blindness appears earlier in life than in patients with USH type 2 (USH2), who tend to have less severe HL and normal vestibular function. In a third classification (USH3), the HL and retinitis pigmentosa (RP) are progressive, with variable vestibular dysfunction. To date, 14 loci have been

mapped for USH in humans, while the genes for only 11 of these loci have been identified.[6] Although variants in each of these genes can cause USH, some variants of *USH* genes are associated only with deafness or only with retinitis pigmentosa.[7–14] However, variants in the reported 11 USH genes do not account for all cases of USH.

The proteins encoded by the reported *USH* genes are present in sensory cells of the inner ear and retina. In vitro and in vivo, multiple molecular interactions have been reported between these USH proteins.[15–18] USH1 and USH2 proteins are thought to be assembled into a complex, with a central scaffold role for the PDZ (PSD-95, Dig, and ZO-1/2) domain-bearing proteins harmonin (USH1C) and whirlin (USH2D).[12151518] Some USH proteins also interact with non-syndromic HL proteins.[161920] Whirlin is cargo of myosin 15[19] and appears to interact with espin,[19] an actin binding and bundling protein. Pathogenic variants of human and mouse *ESPN/Espn* are associated with HL and vestibular dysfunction.[21–23]

Here, we describe a large consanguineous Pakistani family PKDL1051 segregating prelingual sensorineural HL, vestibular dysfunction and progressive impairment of vision. Using a combination of genetic techniques, we identified an inframe deletion encoding six conserved residues in the actin bundling motif of espin that cosegregates with USH1 in family PKDL1051. Our functional analyses revealed that the deletion of the six conserved residues impairs the actin bundling function of purified espin protein. The identification of this inframe deletion in *ESPN* expands phenotypic spectrum of *ESPN* alleles and the repertoire of genetic causes of USH.

MATERIALS AND METHODS

Family ascertainment and clinical evaluations

Written informed consent was obtained from all the participants. We performed medical history interviews to identify possible clinical features of syndromic HL and to rule out potential environmental causes. Hearing was evaluated in audiology clinics by pure tone audiometry at octave frequencies with intensities up to 110 db HL, and vestibular function was evaluated by tandem gait and Romberg testing. Funduscopy and electroretinography (ERG) tests were performed by an ophthalmologist to evaluate the individuals of family PKDF1051 for a vision disorder.

Linkage analysis

Using genomic DNA extracted from peripheral blood samples from affected and unaffected members of family PKDF1051, we screened for linkage of the USH phenotype to short tandem repeat (STR) markers for all of the reported USH loci using a previously described protocol.[24] Genome-wide linkage analysis with homozygosity mapping was performed by using an Illumina 6K linkage array (Illumina, San Diego, California, USA). SNP data with Mendelian inheritance errors, determined by the PedCheck program, was removed from further analysis. Fine mapping and haplotype analyses were performed with STR markers from the chromosome 1 p candidate region. Marker order and map distances are from the Marshfield genetic map. Linkage analysis was performed assuming autosomal recessive inheritance, full penetrance and a disease gene frequency of 0.0001 with equal meiotic

recombination frequencies for males and females. Multipoint and two-point logarithm of the odds (LOD) scores were calculated as described previously.[24]

Candidate gene screening

For mutational screening in the linkage interval, we used the reported intronic primers[22] to specifically PCR amplify and sequence the coding exons and the respective exon–intron boundaries of *ESPN* from the genomic DNA of two affected individuals as described.[22] Cosegregation of the mutation with the phenotype in the family was tested by sequencing exon 11 of *ESPN*. Control DNA samples from an ethnically matched Pakistani population were also sequenced, as described previously,[25] for exon 11 of *ESPN*. Exome sequencing was conducted using a genomic DNA sample from affected member IV: 12 of family PKDF1051.

ESPN expression constructs

Human wild type ESPN ($ESPN^{WT}$) and $ESPN^{p.Lys663ThrfsX1}$ mutant green flourescent protein (GFP)-tagged expression constructs have been described previously.[26] Sequence verified expression constructs encoding $ESPN^{Arg790\text{-}Arg795del}$, $ESPN^{KKEIIK}$, $ESPN^{SQSTTS}$ and other deletions and point mutations in ESPN were prepared through site-directed mutagenesis (Agilent Technologies, Santa Clara, California, USA) using the wild type *ESPN* isoform 3A as a template (nucleotides 1777–2733, GenBank accession number NM_031475).

Cell culture and transfection

LLC-PK1-CL4 cells were grown in Dulbecco's Modified Eagle Medium (DMEM) supplemented with 10% fetal bovine serum, 2mm L-glutamine and penicillin/streptomycin (50U/mL) (Life Technologies, Grand Island, New York, USA) and maintained at 37°C in 5% CO_2. The cells were transfected using Fugene HD Transfection reagent (Promega, Sunnyvale, California, USA) according to the manufacturer's instructions. Cells were then cultured for an additional 24–48 hours prior to immunostaining.

Inner ear explant and gene gun

Inner ear explants were harvested from C57BL/6J mice at postnatal day 1 (P1) to postnatal day 2 (P2). The explants were cultured in a Matrigel coated glass-bottom Petri dish (MatTek, Ashland, Massachusetts, YSA) and were maintained in 7% fetal bovine serum (Life Technologies) supplemented DMEM for 24 hours at 37°C with 5% CO_2. The cultures were transfected using a Helios gene gun (Bio-Rad, Hercules, California, USA) as described elsewhere.[27] The cells were then cultured for an additional 24–48 hours prior to immunostaining.

The stereocilia length was quantified using ImageJ software. Each stereocilium was assimilated to a line (T_1 B_2) with $T_1 = (x_1, y_1, z_1)$ at the tip of the stereocilia and $B_2 = (x_2, y_2, z_2)$ at its base. The stereocilia length $d(T_1B_2)$ was calculated as following:

$$d(T_1, B_2) = \sqrt{(x_2 - x_1)^2 + (y_2 - y_1)^2 + (z_2 - z_1)^2}$$

A minimum of 15 stereocilia (n≥15) from three different cells were quantified.

Actin binding and bundling assays

Recombinant N-terminally 6xHis-tagged human espin 3A proteins, wild type and mutant, were expressed in *Escherichia coli* BL21 (DE3) cells using the Invitrogen ProEX-HTa vector and purified as described previously.[28] Cosedimentation actin-binding assays and actin-bundling assays were carried out as described previously,[29] except HEPES substituted for imidazole as the buffer. Rabbit skeletal muscle actin was obtained from Cytoskeleton (AKL99).

RESULTS

Clinical description

At the time of examination, the ages of the affected individuals in family PKDF1051 (figure 1A) ranged from 21 years to 42 years. All affected individuals were said to have prelingual bilateral profound sensorineural HL (figure 1B) and delayed onset (≥2.5 years) of independent ambulation, consistent with a vestibular dysfunction, which was further confirmed by tandem gait ability and by using the Romberg test. All of the affected individuals complained about night vision problems. Therefore, we performed funduscopy and ERG tests to characterise their vision. Funduscopic examination of affected individuals of family PKDF1051 revealed an irregular retinal contour, temporal lipofuscin flecks and disc pallor in both eyes with normal retinal vessels (figure 2, table 1). ERG revealed both diminished scotopic rod and scotopic combined responses among affected individuals with a relative preservation of photopic responses (figure 3, online supplementary table S1), which may reflect very early rod photoreceptor disorder (eg, USH and incomplete stationary night blindness). Electrocardiography revealed left ventricular hypertrophy in two of the five affected individuals evaluated (table 1). Serum biochemistry suggests intact kidney and liver function among the affected individuals (table 1). Similarly, urinalysis did not reveal any obvious pathologies in the affected individuals, except for frequent uric acid crystals. Taken together, these clinical evaluations indicate prelingual, sensorineural profound HL, vestibular dysfunction and late onset, progressive vision impairment—a phenotype consistent with USH type I.

Linkage mapping and candidate gene screening

Next, to understand the genetic deficit responsible for an USH phenotype segregating in family PKDF1051, we screened with genetic markers for linkage to the known *USH* loci/genes.[30] After excluding linkage to all of the reported *USH* loci, we undertook a genome-wide screen using an Illumina SNP 6K linkage panel and genomic DNA samples from family PKDF1051, which showed suggestive evidence of linkage to markers on chromosome 1p36.32-p36.22. Affected individuals were homozygous for markers in this interval, while unaffected obligate carriers were heterozygous. Haplotype analysis using STR markers revealed a 9.83 cM interval of homozygosity delimited by markers *D1S2660* (10.78 cM) and *D1S450* (20.61 cM; figure 1A). A maximum two-point lod score (Z_{max}) of 3.79 at recombination fraction θ=0 was obtained for the marker *D1S214* (online supplementary table S2). Considering the clinical phenotype, the Human Genome

Organisation (HUGO) gene nomenclature committee assigned an *USH1M* as the designation for this *USH* locus defined by family PKDF1051.

Based on Human Genome Assembly GRCh37 (hg19), the *USH1M* locus has 54 annotated and hypothetical genes located in an approximately 4.78 Mb interval. The *USH1M* critical interval also overlaps with *DFNB36* (MIM 609006), a locus for non-syndromic recessively HL with vestibular dysfunction, for which mutations in *ESPN* were reported (figure 1E).[22] Heterozygous alleles of *ESPN* are also known to cause dominantly inherited HL in humans (figure 1E).[21] Similarly, in *jerker* mouse, loss-of-function *Espn* alleles are known to cause deafness, hyperactivity and circling behaviour.[23] Therefore, we considered the possibility that a homozygous variant of *ESPN* might underlie the USH1M phenotype as well. All the coding and non-coding exons of the *ESPN* gene were Sanger sequenced in affected individuals VI:10 and VI:12 (figure 1A). We identified a novel homozygous 18 base pair (bp) deletion (c.2369_2386delAGGCGGGACCTCCTGCGG) within exon 11 (figure 1C) of *ESPN*, which cosegregated with the phenotype in family PKDF1051. Human chromosome 1 p also harbours an unprocessed *ESPN* partial gene *(ESPNP;* GenBank Accession #AL035288), which has 95% identity with *ESPN*.[22] To unambiguously assign the presence of the 18 bp deletion to the *ESPN* gene, we subcloned the *ESPN* exon 11 PCR fragment and sequenced individual clones. The *ESPN* and *ESPNP* clones were separated based on the nucleotide mismatches within exon 11. The 18 bp deletion was only observed in the *ESPN* specific exon 11 and not in the *ESPNP* gene. Inframe deletion of these 18 nucleotides is predicted to remove six conserved residues (p.790_795delRRDLLR), including three positively charged arginines, from the actin-bundling motif of encoded espin protein (figure 1D,E). Carriers of c.2369_2386del18bp were not identified among 224 ethnically matched control chromosomes in over 65 000 individuals listed in ExAC database or in the 6500 individuals NHLBI-ESP variant database.[3132]

To further confirm that the *ESPN* variant is the only pathogenic change within the linkage region as well as across the genome that is cosegregating with USH1 phenotype in family PKDF1051, we performed whole exome sequencing (WES) on affected individual VI:12. All variants found in the WES data are summarised in online supplementary table S3. Bioinformatics and segregation analyses revealed that only the c. 2369_2386delAGGCGGGACCTCCTGCGG variant in *ESPN* cosegregated with the USH1 phenotype in family PKDF1051. WES data did not reveal other potential pathogenic variants shared among affected individuals, except for the 18 bp inframe deletion in *ESPN* at *USH1M* locus (online supplementary table S3). Thus, the WES results support the supposition that the USH1 phenotype in family PKDF1051 is due to a recessive inframe deletion in *ESPN* at the *USH1M* locus.

USH1M variant impairs the actin-bundling ability of espin

In humans, the full-length *ESPN* isoform encodes a polypeptide of 854 amino acids, with eight predicted ankyrin-like repeats, two proline-rich domains, a WH2 motif and an actin bundling motif (figure 1E). Deletion mutagenesis experiments indicate that espin contains two actin-binding sites within the actin-bundling domain.[28] Although the *USH1M* variant of *ESPN* is not part of either actin binding site, it is predicted to remove six evolutionarily

conserved residues (online supplementary figure S1) from the intervening region between 786 and 801.

To determine the effect of the *USH1M* variant on the function of espin, we capitalised on the protein's known microvillar targeting and elongation activities in heterologous epithelial cells, which are mediated by the actin-binding motif.[26] Our transiently transfected GFP-tagged wild type espin 3A isoform was efficiently targeted to the microvilli on the cell apical surface of LLC-PK1-CL4 epithelial cells and elongated them (figure 4A–C and P), as reported previously.[26] The construct bearing, the p.Lys663Thrfs*1, a known *DFNB36* allele of *ESPN* missing the actin-binding motif,[22] failed to target or elongate microvilli in the transfected LLC-PL1-CL4 cells (figure 4D–F and P). In contrast, the *ESPN* construct bearing the *USH1M* variant (p.790_795delRRDLLR) resulted in a protein that retained microvillar targeting ability but lacked microvillar elongation activity (figure 4G–I and P). The bulk of this mutated espin was detected in the cytoplasm, nucleus and junctional belt at the cell periphery (figure 4G,H and P). Microvillar elongation ability is believed to stem directly from espin's actin cross linking ability,[33] which seems to be affected by the *USH1M* variant.

There are several possible explanations for the p.790_795delRRDTTR variant's effect on the espin protein, including the contribution of the deleted specific residues in protein structure and function, the necessity of positively charged residues at these positions or the requirement of these six amino acids to set the correct spacing between F-actin-binding sites. To address this question, we replaced the six conserved amino acids at positions at 790–795 with six alternative charged and hydrophobic amino acids, p.KKEIIK, in the same pattern. When transiently transfected in LLC-PK1-CL4 cells, the ESPN^{KKEIIK} protein was efficiently targeted to the microvilli on the cell surface of LLC-PK1-CL4 cells and elongated them (figure 4J–L and P). However, when the p.790–795 residues of espin were replaced with a specific sequence of neutral amino acids (p.SQSTTS), the resulting protein (online supplementary figure S2) failed to be targeted to microvilli or the cellular junctional belt at the cell periphery (figure 4M–O and P). These functional studies suggest that the six residue peptide, p.RRDLLR, with its characteristic placement of charged and hydrophobic residues, is essential for the stability and actin bundling function of espin.[33] We also evaluated the effect of replacing or deleting single, double or triple residues between positions 790–795 for their effect on microvilli elongation in LLC-PK1-CL4 cells. Even a single amino acid substitution or deletion at positions 790–795 resulted in the loss of microvillar elongation activity (online supplementary figure S3), further highlighting the importance of the positively charged amino acids in this sequence.

Next, to determine the effect of the *USH1M* variant (p.790_795delRRDLLR) on espin function in mouse inner ear sensory hair cells, we used an in vivo targeting and localisation assay. Using a Helios gene gun, we transfected wild type p.Lys663Thrfs*1 (DFNB36 variant) and p.790_795delRRDLLR mutant GFP-tagged *ESPN* cDNA constructs into organotypic cultures of inner ear sensory epithelia of P1 to P2 C57BL/6J mice (figure 5). Overexpressed wild type GFP-espin localised along the length of the stereocilia in cochlear hair cells and caused their overelongation (figure 5A,B and I,J), as previously reported.[33] Similar to the results that were observed in LLC-PK1-CL4 cells, the ESPN^{KKEIIK} protein

was efficiently targeted to the stereocilia of hair cells and elongated them (figure 5C,D and I,J). In contrast, GFP–espin harbouring the p.Lys663Thrfs*one variant failed to target to stereocilia, and the protein was apparently distributed throughout cochlear hair cell bodies (figure 5E,F and I,J). The GFP–espin with the *USH1M* variant (p.790_795delRRDLLR) localised along the length of the stereocilia of cochlear hair cells but failed to overelongate them (figure 5G,H and I,J). These results support the conclusion that the *USH1M* variant in the actin-bundling motif likely affects its function in stereocilia.

Finally, we used standard F-actin cosedimentation assays to demonstrate that espin harbouring the p.790_795delRRDLLR deletion retained residual binding to F-actin but has impaired bundling function. For the F-actin-binding assays, purified wild type or p.790_795delRRDLLR deletion-harbouring espin 3A were incubated with polymerised rabbit F-actin and subjected to high-speed centrifugation at 150 000×*g* for 60 min (figure 5K), a condition known to pellet the F-actin. A large fraction (~45%) of the wild type espin 3A cosedimented with F-actin in the pellet but not in the absence of actin (figure 5K). Relative to wild type, the espin 3A with the p.790-795delRRDLLR mutation showed reduced (~15%) binding to F-actin, but the binding was significantly higher than background. When actin-bundling function was evaluated under a reduced centrifugation speed and time (22 000×*g* for 15 min), wild type espin was able to bundle the F-actin, which ended up in the pellet (figure 5L). By contrast, the espin with USH1M deletion remained in the supernatant and failed to shift actin filaments from the supernatant to pellet (figure 5L), further confirming an impaired actin bundling function.

DISCUSSION

Our study provides genetic evidence of an association of a six-amino acid deletion variant (p.790_795del RRDLLR) of *ESPN* segregating in a large human family (22 affected individuals) with USH type 1M characterised by deafness, vestibular areflexia and progressive vision impairment. *ESPN* encodes several alternatively spliced transcripts that encode actin binding and bundling proteins necessary for inner ear hair cell stereocilia.[282933] Our functional studies revealed that deletion of this six-residue block, which includes three arginine residues, significantly attenuates the actin bundling function of espin in cells and in vitro.

Recessive variants, including truncations (figure 1E) of *ESPN*, were previously reported to be associated only with prelingual HL (DFNB36) and vestibular areflexia.[22] Vision impairment was not reported among the affected individuals of these families. In contrast, all five affected individuals of the PKDF1051 family, evaluated by an ophthalmologist, have progressive retinal abnormalities and vision impairment that include temporal flecks, pallor disc and reduced scotopic ERG responses. Greatly diminished rod-based scotopic ERG wave amplitudes are consistent with early signs of retinitis pigmentosa. The presence of HL, vestibular areflexia and retinitis pigmentosa are consistent with classification as USH. As all of these features are present in the five affected individuals of family PKDF1051 that were evaluated by an ophthalmologist, therefore, we categorised their phenotype as USH.

USH is classified into three clinical subtypes: USH1, USH2 and USH3.[6] However, atypical forms of USH have been observed in patients harbouring mutant alleles in known *USH1* and *USH2* genes. For instance, mutant alleles of *MYO7A* are the most frequent cause of USH1 in the US population. Although rare, certain alleles of *MYO7A* have also been associated with the USH2 phenotype with normal vestibular functions in humans. Similarly, *CDH23* (USH1D), *USH2A* (USH2A) and *SANS* (USH1G) alleles have been associated with atypical forms of USH.[34] Funduscopic features of patients with USH1 include attenuated vessels and intraretinal pigment migration in the form of bone spicules or pigment clumps, which we did not observe among the affected individuals of family PKDF1051. Also, ERG can be abnormal as early as infancy in patients with USH1, with a decline in rod and cone responses and implicit times.[6] Considering the largely intact cone function in a 42-year-old deaf individual (VI: 12), the absence of bone spicules and the attenuated blood vessel, we categorise the affected individuals of PKDF1051 as an atypical form of USH1.

There are several possibilities that may account for the USH phenotype segregating in family PKDF1051 and the non-syndromic deafness segregating in DFNB36 families. First, affected individuals of DFNB36 families were evaluated by ERG for visual deficits when they were young (14 years and 19 years), while affected individuals of PKDF1051 are 30–42 years old. Second, in contrast to the previously reported truncating and presumably loss-of-function alleles found in DFNB36 families, the inframe six-amino acid deletion segregating in family PKDF1051 may be a gain-of-function recessive allele that hampers retinal and inner ear function. Third, another pathogenic variant of neighbouring gene-causing RP in the five clinically evaluated affected individuals of family PKDF1051 might be in linkage disequilibrium with the inframe deletion of *ESPN*. However, further analysis of the WES results of affected individual IV:12 of family PKDF1051 for chromosome 1 did not reveal any other potential pathogenic variant within the *USH1M* linkage interval (online supplementary table S4). Finally, we also cannot entirely rule out genetic, stochastic and environmental factors contributing to the differences in phenotypes between DFNB36 and USH1M.

Growing evidence suggests that in the inner ear, USH proteins are components of tip links that interconnect stereocilia and convey mechanical forces to the mechanoelectrical transduction machinery, the stereocilia ankle links and side links and are necessary for stereocilia elongation and synaptic functions.[35–44] In the retina, USH proteins colocalise in the synaptic layer as well as in the ciliary region between the outer and inner segments, more particularly in the connecting cilium and the calyceal processes.[45] In the mouse retina, espin is expressed in the retina and partially colocalises with whirlin (USH2D) in the inner segment and synaptic termini of mouse photoreceptors[20] suggesting a function of espin in the retina. In vitro, mouse espin was found to interact with mouse whirlin in yeast two-hybrid assays and by coimmunoprecipitation from cotransfected cultured cells, and thus was proposed as a candidate gene for USH2 in humans.[19] Our studies provide the first genetic evidence of espin's important role in the retina and an association with USH.

Supplementary Material

Refer to Web version on PubMed Central for supplementary material.

Acknowledgements

We are very grateful to family members who participated in the study. We thank Dr Arnaud Giese for his help in preparing figures, technical assistance and discussions of the results.

Funding This study has been supported by grants from: the National Institutes of Health (NIH) – National Institute on Deafness and Other Communication Disorders (NIDCD) R56DC011803, R01DC016295 (to SaR and ZMA) and R01DC004314 (to JRB). This work was supported (in part) by NIDCD/NIH Intramural Program funds DC000039-15 (to TBF).

REFERENCES

1. Scheffer DI, Shen J, Corey DP, Chen ZY. Gene Expression by Mouse Inner Ear Hair Cells during Development. J Neurosci 2015;35:6366–80. [PubMed: 25904789]
2. Admiraal RJ, Huygen PL. Changes in the aetiology of hearing impairment in deaf-blind pupils and deaf infant pupils at an institute for the deaf. Int J Pediatr Otorhinolaryngol 2000;55:133–42. [PubMed: 11006453]
3. Armitage IM, Burke JP, Buffin JT. Visual impairment in severe and profound sensorineural deafness. Arch Dis Child 1995;73:53–6. [PubMed: 7639551]
4. Nicoll AM, House P. Ocular abnormalities in deaf children: a discussion of deafness and retinal pigment changes. Aust N Z J Ophthalmol 1988;16:205–8. [PubMed: 3179048]
5. Kimberling WJ, Hildebrand MS, Shearer AE, Jensen ML, Halder JA, Trzupek K, Cohn ES, Weleber RG, Stone EM, Smith RJ. Frequency of Usher syndrome in two pediatric populations: Implications for genetic screening of deaf and hard of hearing children. Genet Med 2010;12:512–6. [PubMed: 20613545]
6. Friedman TB, Schultz JM, Ahmed ZM, Tsilou ET, Brewer CC. Usher syndrome: hearing loss with vision loss. Adv Otorhinolaryngol 2011;70:56–65. [PubMed: 21358186]
7. Ahmed ZM, Riazuddin S, Ahmad J, Bernstein SL, Guo Y, Sabar MF, Sieving P, Riazuddin S, Griffith AJ, Friedman TB, Belyantseva IA, Wilcox ER. PCDH15 is expressed in the neurosensory epithelium of the eye and ear and mutant alleles are responsible for both USH1F and DFNB23. Hum Mol Genet 2003;12:3215–23. [PubMed: 14570705]
8. Ahmed ZM, Riazuddin S, Aye S, Ali RA, Venselaar H, Anwar S, Belyantseva PP, Qasim M, Riazuddin S, Friedman TB. Gene structure and mutant alleles of PCDH15: nonsyndromic deafness DFNB23 and type 1 Usher syndrome. Hum Genet 2008;124:215–23. [PubMed: 18719945]
9. Astuto LM, Bork JM, Weston MD, Askew JW, Fields RR, Orten DJ, Ohliger SJ, Riazuddin S, Morell RJ, Khan S, Riazuddin S, Kremer H, van Hauwe P, Moller CG, Cremers CW, Ayuso C, Heckenlively JR, Rohrschneider K, Spandau U, Greenberg J, Ramesar R, Reardon W, Bitoun P, Millan J, Legge R, Friedman TB, Kimberling WJ. CDH23 mutation and phenotype heterogeneity: a profile of 107 diverse families with Usher syndrome and nonsyndromic deafness. Am J Hum Genet 2002;71:262–75. [PubMed: 12075507]
10. Bork JM, Peters LM, Riazuddin S, Bernstein SL, Ahmed ZM, Ness SL, Polomeno R, Ramesh A, Schloss M, Srisailpathy CR, Wayne S, Bellman S, Desmukh D, Ahmed Z, Khan SN, Kaloustian VM, Li XC, Lalwani A, Riazuddin S, Bitner-Glindzicz M, Nance WE, Liu XZ, Wistow G, Smith RJ, Griffith AJ, Wilcox ER, Friedman TB, Morell RJ. Usher syndrome 1D and nonsyndromic autosomal recessive deafness DFNB12 are caused by allelic mutations of the novel cadherin-like gene CDH23. Am J Hum Genet 2001;68:26–37. [PubMed: 11090341]
11. Doucette L, Merner ND, Cooke S, Ives E, Galutira D, Walsh V, Walsh T, MacLaren L, Cater T, Fernandez B, Green JS, Wilcox ER, Shotland Li, Shotland L, Li XC, Li XC, Lee M, King MC, Young TL, Xc L, Profound YTL. Profound, prelingual nonsyndromic deafness maps to chromosome 10q21 and is caused by a novel missense mutation in the Usher syndrome type iF gene PCDH15. Eur J Hum Genet 2009;17:554–64. [PubMed: 19107147]
12. Riazuddin S, Belyantseva IA, Giese AP, Lee K, Indzhykulian AA, Nandamuri SP, Yousaf R, Sinha GP, Lee S, Terrell D, Hegde RS, Ali RA, Anwar S, Andrade-Elizondo PB, Sirmaci A, Parise LV, Basit S, Wali A, Ayub M, Ansar M, Ahmad W, Khan SN, Akram J, Tekin M, Riazuddin S, Cook T, Buschbeck EK, Frolenkov GI, Leal SM, Friedman TB, Ahmed ZM. Alterations of the CIB2

calcium- and integrin-binding protein cause Usher syndrome type 1J and nonsyndromic deafness DFNB48. Nat Genet 2012;44:1265–71. [PubMed: 23023331]

13. Riazuddin S, Nazli S, Ahmed ZM, Yang Y, Zulfiqar F, Shaikh RS, Zafar AU, Khan SN, Sabar F, Javid FT, Wilcox ER, Tsilou E, Boger ET, Sellers JR, Belyantseva IA, Riazuddin S, Friedman TB. Mutation spectrum of MYO7A and evaluation of a novel nonsyndromic deafness DFNB2 allele with residual function. Hum Mutat 2008;29:502–1 1. [PubMed: 18181211]
14. Xu W, Dai H, Lu T, Zhang X, Dong B, Li Y. Seven novel mutations in the long isoform of the USH2A gene in Chinese families with nonsyndromic retinitis pigmentosa and Usher syndrome Type II. Mol Vis 2011;17:1537–52. [PubMed: 21686329]
15. Adato A, Michel V, Kikkawa Y, Reiners J, Alagramam KN, Weil D, Yonekawa H, Wolfrum U, El-Amraoui A, Petit C. Interactions in the network of Usher syndrome type 1 proteins. Hum Mol Genet 2005;14:347–56. [PubMed: 15590703]
16. Kremer H, van Wijk E, Märker T, Wolfrum U, Roepman R. Usher syndrome: molecular links of pathogenesis, proteins and pathways. Hum Mol Genet 2006;15(Spec No 2):R262–R270. [PubMed: 16987892]
17. Sahly I, Dufour E, Schietroma C, Michel V, Bahloul A, Perfettini I, Pepermans E, Estivalet A, Carette D, Aghaie A, Ebermann I, Lelli A, Iribarne M, Hardelin JP, Weil D, Sahel JA, El-Amraoui A, Petit C. Localization of Usher 1 proteins to the photoreceptor calyceal processes, which are absent from mice. J Cell Biol 2012;199:381–99. [PubMed: 23045546]
18. van Wijk E, van der Zwaag B, Peters T, Zimmermann U, Te Brinke H, Kersten FF, Märker T, Aller E, Hoefsloot LH, Cremers CW, Cremers FP, Wolfrum U, Knipper M, Roepman R, Kremer H. The DFNB31 gene product whirlin connects to the Usher protein network in the cochlea and retina by direct association with USH2A and VLGR1. Hum Mol Genet 2006;15:751–65. [PubMed: 16434480]
19. Belyantseva IA, Boger ET, Naz S, Frolenkov GI, Sellers JR, Ahmed ZM, Griffith AJ, Friedman TB. Myosin-XVa is required for tip localization of whirlin and differential elongation of hair-cell stereocilia. Nat Cell Biol 2005;7:148–56. [PubMed: 15654330]
20. Wang L, Zou J, Shen Z, Song E, Yang J. Whirlin interacts with espin and modulates its actin-regulatory function: an insight into the mechanism of Usher syndrome type II. Hum Mol Genet 2012; 21:692–710. [PubMed: 22048959]
21. Donaudy F, Zheng F, Ficarella R, Ballana E, Carella M, Melchionda S, Estivill X, Bartles JR, Gasparini P. Espin gene (ESPN) mutations associated with autosomal dominant hearing loss cause defects in microvillar elongation or organisation. J Med Genet 2006;43:157–61. [PubMed: 15930085]
22. Naz S, Griffith AJ, Riazuddin S, Hampton LL, Battey JF, Khan SN, Riazuddin S, Wilcox ER, Friedman TB. Mutations of ESPN cause autosomal recessive deafness and vestibular dysfunction. J Med Genet 2004;41:591–5. [PubMed: 15286153]
23. Zheng L, Sekerková G, Vranich K, Tilney LG, Mugnaini E, Bartles JR. The deaf jerker mouse has a mutation in the gene encoding the espin actin-bundling proteins of hair cell stereocilia and lacks espins. Cell 2000;102:377–85. [PubMed: 10975527]
24. Ahmed ZM, Riazuddin S, Bernstein SL, Ahmed Z, Khan S, Griffith AJ, Morell RJ, Friedman TB, Riazuddin S, Wilcox ER. Mutations of the protocadherin gene PCDH15 cause Usher syndrome type 1F. Am J Hum Genet 2001;69:25–34. [PubMed: 11398101]
25. Riazuddin S, Hussain M, Razzaq A, Iqbal Z, Shahzad M, Polla DL, Song Y, van Beusekom E, Khan AA, Tomas-Roca L, Rashid M, Zahoor MY, Wissink-Findhout WM, Basra MAR, Ansar M, Agha Z, van Heeswijk K, Rasheed F, Van de Vorst M, Veltman JA, Gilissen C, Akram J, Kleefstra T, Assir MZ, Uk 1OK, Grozeva D, Carss K, Raymond FL, O'Connor TD, Riazuddin SA, Khan SN, Ahmed ZM, de Brouwer APM, van Bokhoven H, Riazuddin S. Exome sequencing of Pakistani consanguineous families identifies 30 novel candidate genes for recessive intellectual disability. Mol Psychiatry 2017;22:1604–14. [PubMed: 27457812]
26. Zheng L, Zheng J, Whitlon DS, Garía-Añoveros J, Bartles JR. Targeting of the hair cell proteins cadherin 23, harmonin, myosin XVa, espin, and prestin in an epithelial cell model. J Neurosci 2010;30:7187–201. [PubMed: 20505086]
27. Nayak G, Lee SI, Yousaf R, Edelmann SE, Trincot C, Van Itallie CM, Sinha GP, Rafeeq M, Jones SM, Belyantseva IA, Anderson JM, Forge A, Frolenkov GI, Riazuddin S. Tricellulin deficiency

affects tight junction architecture and cochlear hair cells. J Clin Invest 2013;123:4036–49. [PubMed: 23979167]

28. Zheng L, Beeler DM, Bartles JR. Characterization and regulation of an additional actin-filament-binding site in large isoforms of the stereocilia actin-bundling protein espin. J Cell Sci 2014;127(Pt 6)1306–17. [PubMed: 24424026]
29. Chen B, Li A, Wang D, Wang M, Zheng L, Bartles JR. Espin contains an additional actin-binding site in its N terminus and is a major actin-bundling protein of the Sertoli cell-spermatid ectoplasmic specialization junctional plaque. Mol Biol Cell 1999;10:4327–39. [PubMed: 10588661]
30. Koffler T, Ushakov K.Avraham KB. Genetics of Hearing Loss: Syndromic. Otolaryngol Clin North Am 2015;48:1041–61. [PubMed: 26443487]
31. Fu W, O'Connor TD, Jun G, Kang HM.Abecasis G, Leal SM, Gabriel S, Rieder MJ, Altshuler D, Shendure J, Nickerson DA, Bamshad MJ, Akey JM; NHFBI Exome Sequencing Project. Analysis of 6,515 exomes reveals the recent origin of most human protein-coding variants. Nature 2013;493:216–20. [PubMed: 23201682]
32. Lek M, Karczewski KJ, Minikel EV, Samocha KE, Banks E, Fennell T, O'Donnell-Luria AH, Ware JS, Hill AJ, Cummings BB, Tukiainen T, Birnbaum DP, Kosmicki JA, Duncan LE, Estrada K, Zhao F, Zou J, Pierce-Hoffman E, Berghout J, Cooper DN, Deflaux N, DePristo M, Do R, Flannick J, Fromer M, Gauthier L, Goldstein J, Gupta N, Howrigan D, Kiezun A, Kurki MI, Moonshine AL, Natarajan P, Orozco L, Peloso GM, Poplin R, Rivas MA, Ruano-Rubio V, Rose SA, Ruderfer DM, Shakir K, Stenson PD, Stevens C, Thomas BP, Tiao G, Tusie-Funa MT, Weisburd B, Won HH, Yu D, Altshuler DM, Ardissino D, Boehnke M, Danesh J, Donnelly S, Elosua R, Florez JC, Gabriel SB, Getz G, Glatt SJ, Hultman CM, Kathiresan S, Laakso M, McCarroll S, McCarthy MI, McGovern D, McPherson R, Neale BM, Palotie A, Purcell SM, Saleheen D, Scharf JM, Sklar P, Sullivan PF, Tuomilehto J, Tsuang MT, Watkins HC, Wilson JG, Daly MJ, MacArthur DG, Exome Aggregation C; Exome Aggregation Consortium. Analysis of protein-coding genetic variation in 60,706 humans. Nature 2016;536:285–91. [PubMed: 27535533]
33. Loomis PA, Zheng L, Sekerková G, Changyaleket B, Mugnaini E, Bartles JR. Espin cross-links cause the elongation of microvillus-type parallel actin bundles in vivo. J Cell Biol 2003; 163:1045–55. [PubMed: 14657236]
34. Jiang L, Liang X, Li Y, Wang J, Zaneveld JE, Wang H, Xu S, Wang K, Wang B, Chen R, Sui R. Comprehensive molecular diagnosis of 67 Chinese Usher syndrome probands: high rate of ethnicity specific mutations in Chinese USH patients. Orphanet J Rare Dis 201540:110.
35. Ahmed ZM, Goodyear R, Riazuddin S, Lagziel A, Legan PK, Behra M, Burgess SM, Lilley KS, Wilcox ER, Riazuddin S, Griffith AJ, Frolenkov GI, Belyantseva IA, Richardson GP, Friedman TB. The tip-link antigen, a protein associated with the transduction complex of sensory hair cells, is protocadherin-15. J Neurosci 2006;26:7022–34. [PubMed: 16807332]
36. Giese APJ, Tang YQ, Sinha GP, Bowl MR, Goldring AC, Parker A, Freeman MJ, Brown SDM, Riazuddin S, Fettiplace R, Schafer WR, Frolenkov GI, Ahmed ZM. CIB2 interacts with TMC1 and TMC2 and is essential for mechanotransduction in auditory hair cells. Nat Commun 2017;8:43. [PubMed: 28663585]
37. Gillespie PG. Myosin-VIIa and transduction channel tension. Nat Neurosci 2002;5:3–4. [PubMed: 11753408]
38. Goodyear RJ, Forge A, Legan PK, Richardson GP. Asymmetric distribution of cadherin 23 and protocadherin 15 in the kinocilial links of avian sensory hair cells. J Comp Neurol 2010;518:4288–97. [PubMed: 20853507]
39. Grati M, Kachar B. Myosin VIIa and sans localization at stereocilia upper tip-link density implicates these Usher syndrome proteins in mechanotransduction. Proc Natl Acad Sci U S A 2011;108:11476–81. [PubMed: 21709241]
40. Gregory FD, Bryan KE, Pangršič T, Calin-Jageman IE, Moser T, Lee A. Harmonin inhibits presynaptic Cav1.3 Ca^{2+} channels in mouse inner hair cells. Nat Neurosci 2011;14:1109–11. [PubMed: 21822269]

41. Gregory FD, Pangrsic T, Calin-Jageman IE, Moser T, Lee A. Harmonin enhances voltage-dependent facilitation of Cav1.3 channels and synchronous exocytosis in mouse inner hair cells. J Physiol 2013;591:3253–69. [PubMed: 23613530]

42. Grillet N, Xiong W, Reynolds A, Kazmierczak P, Sato T, Lillo C, Dumont RA, Hintermann E, Sczaniecka A, Schwander M, Williams D, Kachar B, Gillespie PG, Müller U. Harmonin mutations cause mechanotransduction defects in cochlear hair cells. Neuron 2009;62:375–87. [PubMed: 19447093]

43. Kazmierczak P, Sakaguchi H, Tokita J, Wilson-Kubalek EM, Milligan RA, Müller U, Kachar B. Cadherin 23 and protocadherin 15 interact to form tip-link filaments in sensoiy hair cells. Nature 2007;449:87–91. [PubMed: 17805295]

44. Kros CJ, Marcotti W, van Netten SM, Self TJ, Libby RT, Brown SD, Richardson GP, Steel KP. Reduced climbing and increased slipping adaptation in cochlear hair cells of mice with Myo7a mutations. Nat Neurosci 2002;5:41–7. [PubMed: 11753415]

45. Sorusch N, Wunderlich K, Bauss K, Nagel-Wolfrum K, Wolfrum U. Usher syndrome protein network functions in the retina and their relation to other retinal ciliopathies. Adv Exp Med Biol 2014;801:527–33. [PubMed: 24664740]

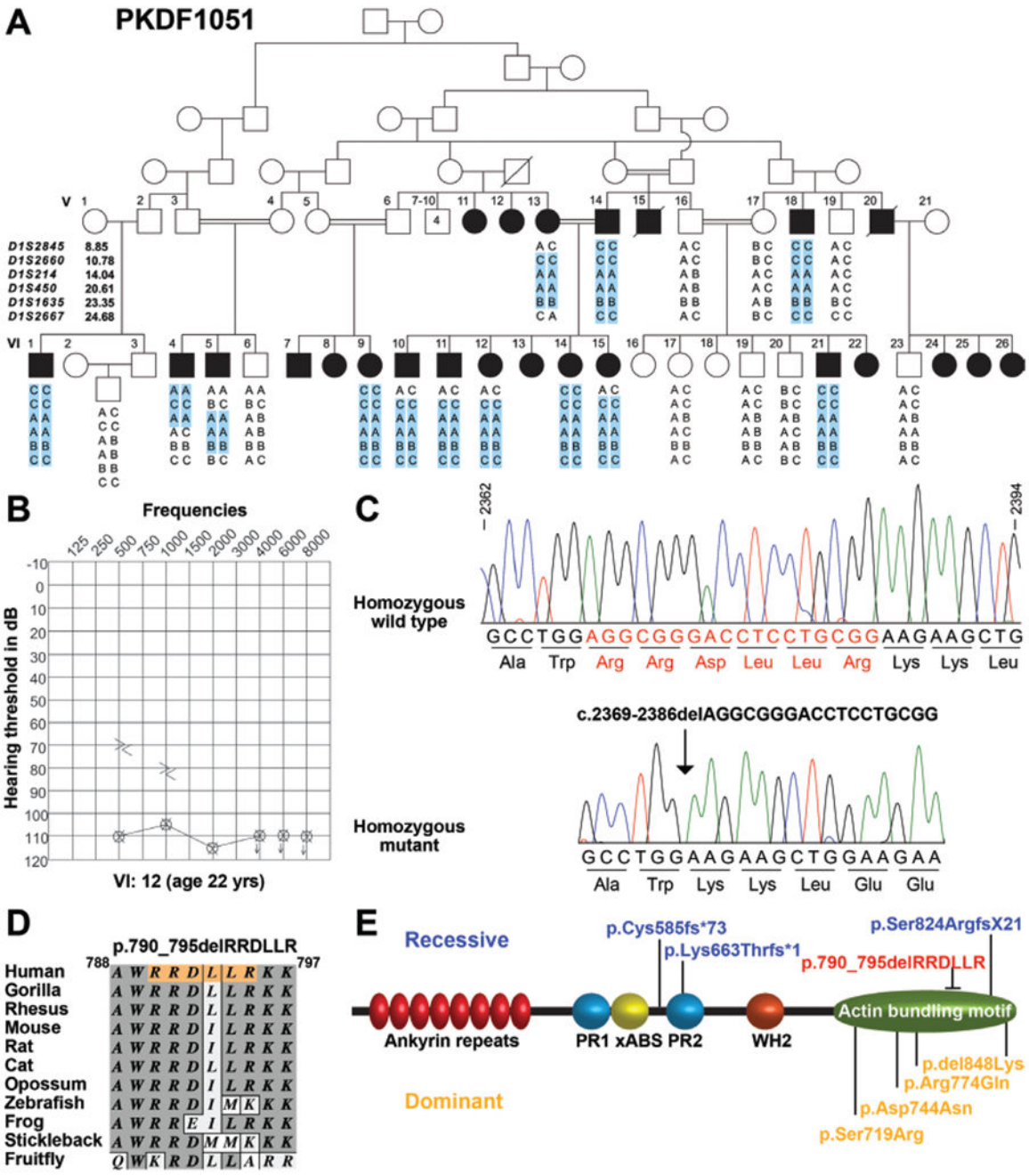

Figure 1.

Family PKDF1051 segregating USH1 shows linkage to markers on chromosome 1 and was designated the *USH1M* locus. Sequencing chromatograms, pure tone audiogram, ClustalW alignment and schematic representation of espin with all of the reported mutations of *ESPN* are shown. (A) Pedigree of family PKDF1051. Filled symbols represent affected individuals. The linked haplotypes are blue coloured. The STR markers and their relative centimorgan (cM) positions, according to the Marshfield genetic map, are shown along with the pedigree. Haplotype of PKDF1051 defines a linkage region of ~9.83 cM delimited by proximal

recombination breakpoint at marker *D1S2660* and distal breakpoint at marker *D1S450* in affected individuals VI:5 and VI:4, respectively. (B) Pure tone air and bone conduction thresholds for family PKDF1051 individual VI:12 (12-year-old female), revealed profound sensorineural hearing loss in both ears. Right ear air conduction: O; left ear air conduction: X; right ear bone conduction: >; left ear bone conduction: <; ↓ indicates the threshold level beyond the measurable range. (C) Homozygous wild type and mutant nucleotide sequencing chromatograms of exon 11 of *ESPN* illustrating the c. 2369_2386delAGGCGGGACCTCCTGCGG variant (arrow). (D) ClustalW multiple sequence alignment of the 10 amino acids of espin shows that p.790_795 residues are conserved across species (shaded background). Amino acids are numbered with reference to GenBank Accession number NP_113663. (E) Mutant alleles causing recessive (blue) and dominant non-syndromic deafness (yellow), and *USH1M* (red) in humans are shown along with the espin protein structure. PR, proline-rich regions; STR, short tandem repeat; xABS, actin-binding sequence; WH2, WASP-homology 2.

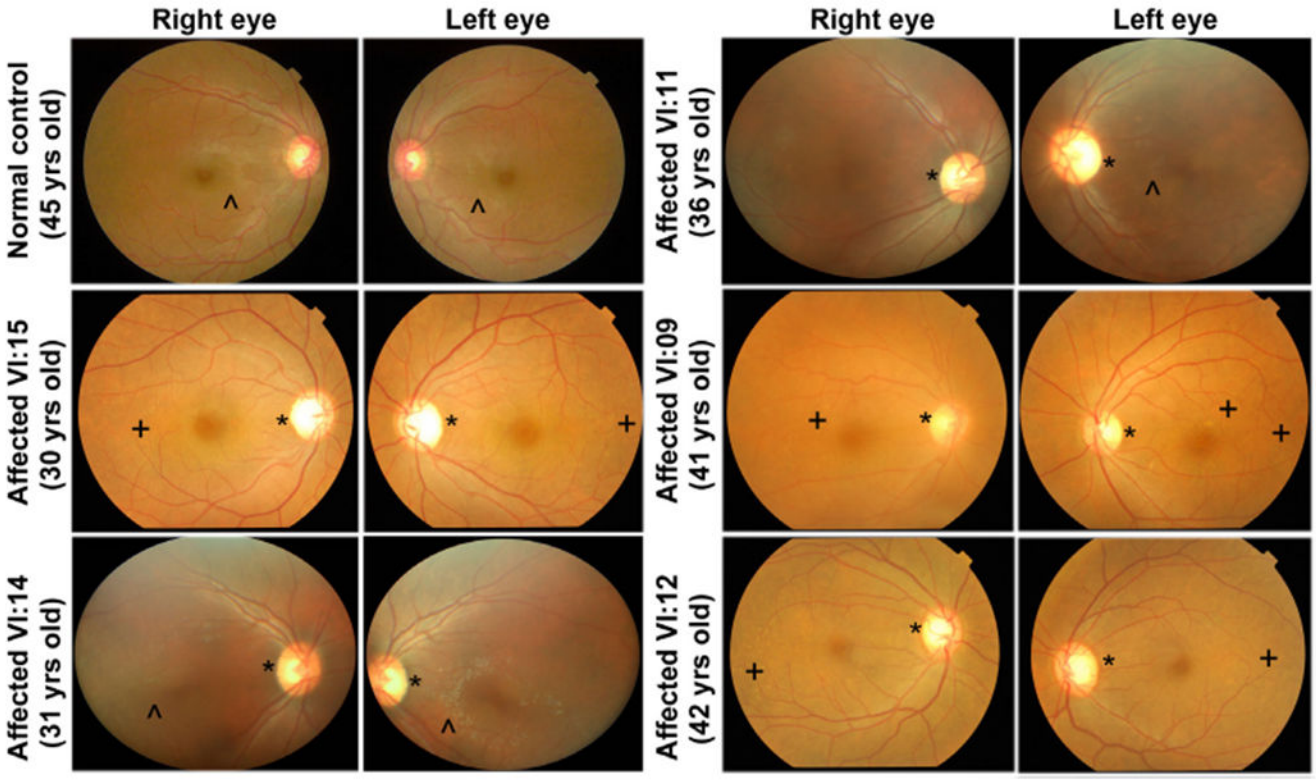

Figure 2.

Funduscopic images revealed signs of retinitis pigmentosa among affected individuals of family PKDF1051. Reduced foveal light reflex was observed among affected individuals. Bilateral symmetrical temporal pallor of the optic disc (*), parafoveal cellophane sheen (^) and temporal and parafoveal drusen (+) were variably present in all affected individuals.

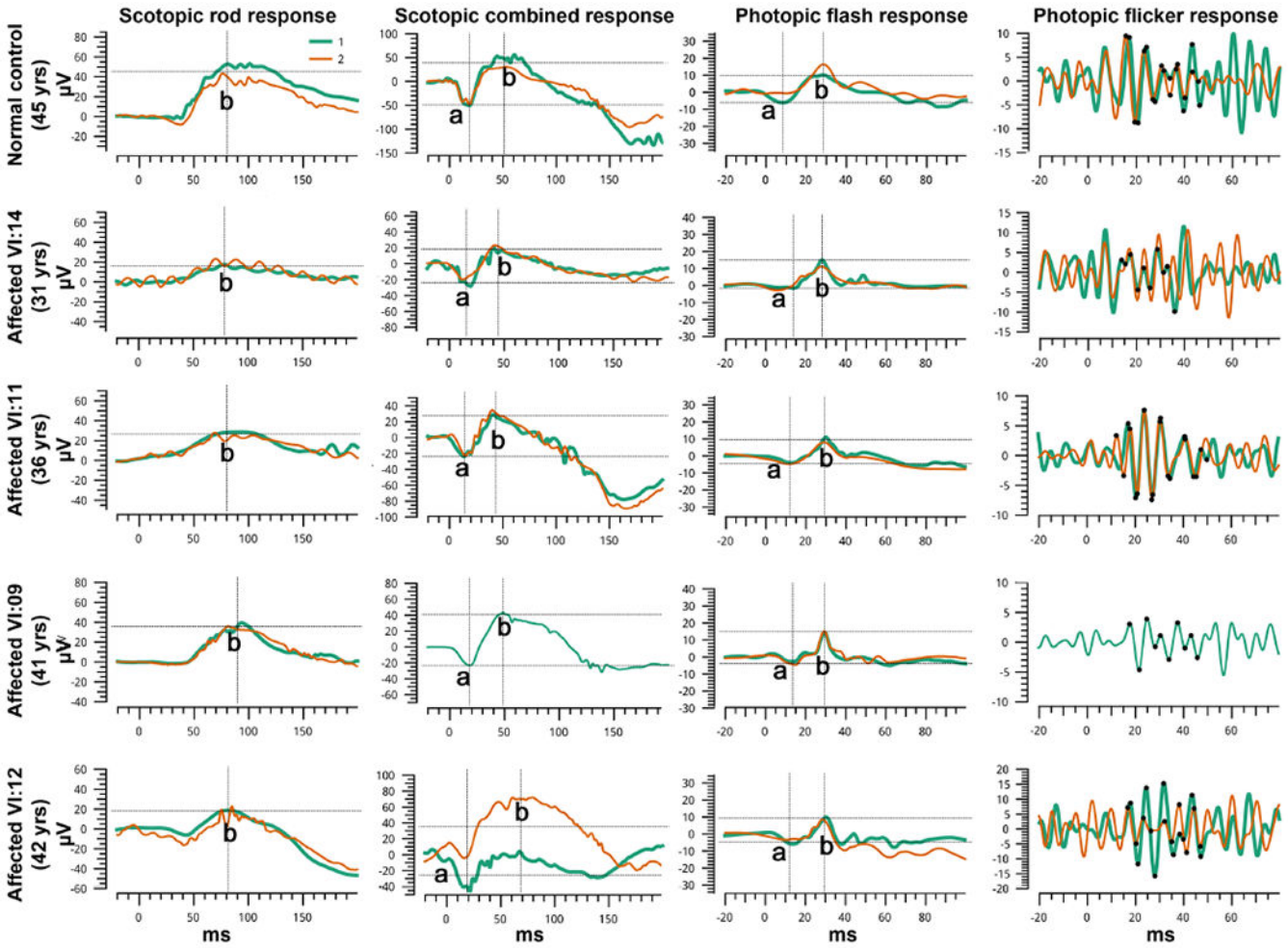

Figure 3.

Full-field electroretinography (ERG) responses for one normal and four oldest affected individuals of family PKDF1051. Two responses (green and orange) have been superimposed for each ERG condition to show reproducibility. The trough of the first negative deflection (first crosshair) represent the a-wave (a). The first positive deflection peak represents the b-wave (b, second cross hair). The amplitude is the difference between the a- and b-wave. Amplitudes were diminished (b-waves greater than a-waves) with preserved implicit times on scotopic rod and scotopic combined responses among affected individuals with relative preservation of photopic responses and oscillatory potentials.

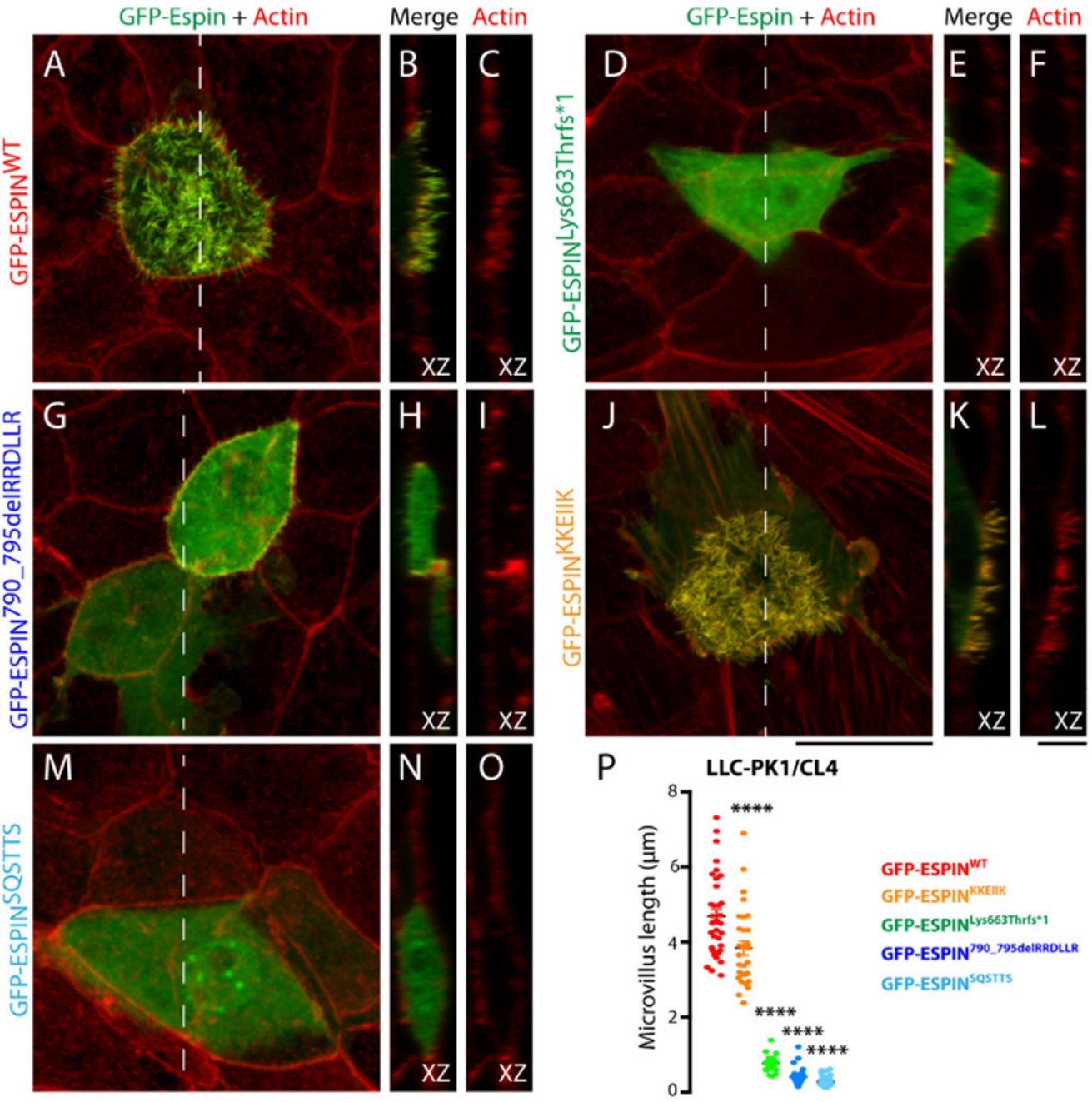

Figure 4.

Functional evaluation of wild type and mutated forms of human GFP-tagged espin using LLC-PK1-CL4 epithelial cells. Actin-based microvilli are labelled with phalloidin (red). (A–C) Wild type GFP–espin was efficiently targeted to microvilli and caused their elongation. (D–F) GFP–espin with the p.Lys663Thrfs*1 (c.1988delAGAG) human *DFNB36* mutation neither targeted microvilli nor caused microvillar elongation and instead was found throughout the cell, including the nucleus. (G–I) GFP–espin with the *USH1M* (p. 790-795delRRDLLR) mutation was found in the cytoplasm, nucleus and the junctional belt

at the cell periphery and did not cause microvillar elongation. (J–O) Replacement of the RRDLLR sequence with KKEIIK (J–L) gave results similar to wild type; however, replacement with the neutral amino acids SQSTTS revealed reduced expression of protein and eliminated microvillar targeting and elongation (M–O). Scale bar in panel O is 10 μm and applies to all panels. (P) Quantification of microvillus length present at the surface of LLC-PK1-CL4 cells transfected with various GFP–espin constructs. ****P<0.005.

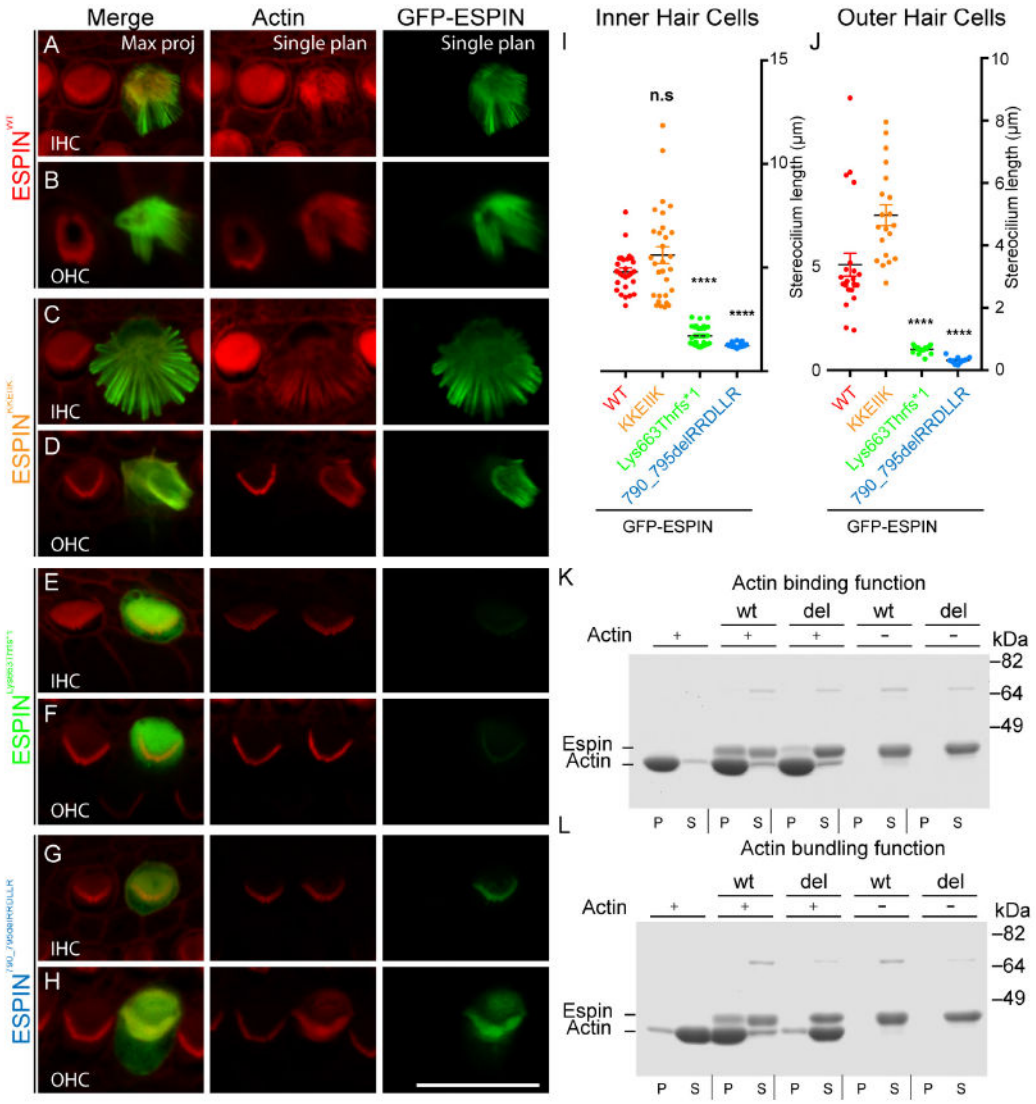

Figure 5.

Analysis of *USH1M* variant using espin-mediated mouse inner ear stereocilia elongation and in vitro actin cosedimentation assays. Mouse hair cell stereocilia were labelled with phalloidin (red). (A and B) Wild type GFP–espin was efficiently targeted to stereocilia actin bundles of inner (A) and outer (B) hair cells (IHCs and OHCs, respectively) and causes their elongation. (C and D) Replacement of the RRDLLR sequence with KKEilK gave results similar to wild type. (E and F) GFP–espin with the *DFNB36* human deafness mutation (p.Lys663Thrfs*1) neither targeted stereocilia nor caused overelongation. (G and H) GFP–espin with the *USH1M* (p.790-795delRRDLLR) mutation was targeted to hair cell stereocilia but did not cause their elongation. Scale bar: 10 µm and applies to all panels. (I and J) Quantification of stereocilia length present at the surface of IHCs (I) and OHCs (J) transfected with various GFP–espin constructs. ****P<0.005. n.s, not significant. (K) Ultracentrifugation F-actin cosedimentation assay with wild type (wt) and *USH1M* mutation (del) revealed cosedimentation of mutant protein with actin in the pellet (P), although less

than wt. S, supernatant. (L) Low speed F-actin bundling assay showing that the *USH1M* mutant (del) protein has reduced actin bundling activity. Most of the actin remained in the S fraction and a very low amount of actin was observed in the pellet compared with the result with wt ESPN.

Table 1

Clinical findings of affected individuals of family PKDF1051

Subject	Normal range	VI:15	VI:14	VI:11	VI:9	VI:12
Sex		F	F	M	F	F
Age (years)		30	31	36	41	42
Genotype		del/del	del/del	del/del	del/del	del/del
Hearing loss		Profound SNHL	Profound SNHL	Profound SNHL	Profound SNHL	Profound SNHL
Vestibular problem *		Yes	Yes	Yes	Yes	Yes
Eye problem						
Funduscopy		Temporal flecks and disc pallor OU	Normal, no disc pallor OU	Rare flecks temporally OU, disc pallor OU	Temporal and parafoveal flecks OU, mild temporal disc pallor OU	Flecks temporally OD>OS, mild temporal disc pallor OD>OS
ERG		NA	Reduced scotopic amplitudes	Reduced amplitudes and prolonged implicit times OU	Reduced scotopic amplitudes (a-waves>b waves)	Slightly reduced amplitudes
OCT		NA	Slightly broad bay of fovea	Thinning of NFL OU	NA	NA
ECG interpretation		Normal	Left ventricular hypertrophy	Left ventricular hypertrophy	Normal	Pericardial effusion
Blood Chemistry						
Sodium	133–145 mmol/L	144	141	138	140	NA
Potassium	3.3–5.1 mmol/L	4.32	3.75	4.55	3.51	NA
Chloride	95–108 mmol/L	105	102	99	102	NA
Bicarbonate	22–29mmol/L	**20.2**	**19.2**	23.1	24.5	NA
Urea nitrogen	6–20 mg/dL	8.5	8.49	10.22	7.27	NA
Creatinine	0.50–0.90 mg/dL	**0.41**	0.5	**0.41**	**0.41**	NA
eGFR	>60mL/min/1.73 m^2	172.68	138.81	170.93	170.1	NA
Total bilirubin	Up to 1.0 mg/dL	0.26	0.18	0.45	0.15	NA
ALT	10–35 U/L	16	25	29	10	NA
AST	10–35 U/L	14	21	18	13	NA
Alkaline phosphatase	35–104 U/L	89	73	92	72	NA
GGT	5–36 U/L	9	7	10	6	NA
Total protein	5.5–8.0 g/dL	7.17	7.69	7.39	6.97	NA

Subject	Normal range	VI:15	VI:14	VI:11	VI:9	VI:12
Albumin (A)	3.5–5.5 g/dL	4.13	4.1	3.62	4.03	NA
Globulin (G)	2.0–3.5 g/dL	3	**3.6**	**3.8**	2.9	NA
A/G ratio		1.36	1.14	0.96	1.37	NA

Given in bold are values outside normal range.

*Evaluated using Romberg and Tandem gait tests.

ALT, alanine aminotransferase; AST, aspartate aminotransferase; eGFR, estimated glomerular filteration rate; ERG, electroretinogram; GGT, gamma-glutamyl transferase; NA, not available; NFL, nerve fiber layer; OCT, optical coherence tomography; OD, oculus dexter (right eye); OS, oculus sinister (left eye); OU, oculus utergue (both eyes); SNHL, sensorineural hearing loss.